Scientific Research Publishing

Optics and Photonics Journal, 2022, 12, 78-87
https://www.scirp.org/journal/opj
ISSN Online: 2160-889X
ISSN Print: 2160-8881

The Effect of Recombination Zone Positon on the Color Temperature Performance in the Color-Tunable White Organic Light-Emitting Diode

Zhixiu Ma*, Ce Bian, Zeyuan Gao

College of Science, University of Shanghai for Science and Technology, Shanghai, China
Email: *mzx2296@163.com

How to cite this paper: Ma, Z.X., Bian, C. and Gao, Z.Y. (2022) The Effect of Recombination Zone Positon on the Color Temperature Performance in the Color-Tunable White Organic Light-Emitting Diode. *Optics and Photonics Journal*, **12**, 78-87.
https://doi.org/10.4236/opj.2022.124006

Received: March 22, 2022
Accepted: April 26, 2022
Published: April 29, 2022

Abstract

Using a color-tunable organic light-emitting diode (CT-OLED) can accord with the circadian cycle of humans and realize healthy lighting. The variation range of the correlated color temperature (CCT) is an important parameter to measure the performance of CT-OLEDs. In this paper, the effect of changing the utilization of phosphorescent materials and the position of the recombination zone (RZ) in the device are investigated by changing the thickness of the emissive layer (EML) and the doping ratio of the host and guest materials. The results show that reducing the red phosphorescent material and improving the blue phosphorescent material can affect the change direction of CCT, but it is not enough to expand the span of CCT (ΔCCT). It is more conducive to improving ΔCCT by more reasonable regulation of the position of the main RZ in EML and the energy transfer from the blue sub-EML to the red sub-EML. Device D obtains the best electro-optic and spectral characteristics, in which the maximum ΔCCT is 5746 K (2661 - 8407 K) as the voltage changes from 3.75 V to 9.75 V, the maximum current efficiency and luminance reach 18.34 cd·A^{-1} and 12,100 cd·m^{-2}, respectively.

Keywords

Optical Devices, Organic Light-Emitting Diode, Color-Tunable, Recombination Zone, Color Temperature

1. Introduction

As a high-efficiency light source, organic light-emitting diode (OLED) has attracted extensive attention in academia and industry because of its high reliabil-

ity, low power consumption, flexibility, and lightweight [1] [2] [3] [4] [5]. Improving the efficiency, lifetime, and reducing production costs of OLED devices have always been important research directions. In addition, people have begun to pay attention to the physiological changes that OLED as an artificial light source brings to humans. It is well known that the correlated color temperature (CCT) of sunlight on earth varies with the time of day (*i.e.* 2500 K at dawn, 3250 K at dusk, 5500 K at noon, and 6500, 8000 K at noon on a cloudy day, in high-latitude countries, respectively) [6], the CCT span (ΔCCT) is about 5500 K (2500 - 8000 K), and the circadian cycle of human and other organisms are closely related to the change of CCT. Therefore, the color-tunable OLED (CT-OLED) with a wide ΔCCT can not only achieve healthy lighting by simulating real sunlight-style lighting, but also improve the additional value of OLED products by extending their application scenario, such as airplane cabin lighting, vegetable planting, and preservation, etc [7] [8] [9] [10].

Since CT-OLED was first proposed by Forrest *et al.* [11], CT-OLEDs prepared by different methods had emerged. As the spectral intensity of a specific wavelength was adjusted by regulating the optical micro-cavity architecture based on metal electrodes with different thickness and morphology or distributed Bragg reflector (DBR) structure, the CCT of the device can be changed, however, which was also fixed when the structure of the device was certain, so it was difficult to achieve the dynamic change of CCT in the working state [12] [13] [14]. In contrast, a vertically stacked CT-OLED can achieve a wide CCT span, but this method was involved with the complicated device structure because it typically required independent voltage to control two or even three light-emitting units, respectively [15] [16] [17] [18] [19]. In addition to the above two methods for preparing CT-OLED, many studies had shown that it was also beneficial to achieve a wider ΔCCT by inserting the carrier modulation layer between different color emissive layers to broaden the area of the carrier recombination zone (RZ) [6] [20] [21]. Xu *et al.* inserted a MADN spacer layer between undoped ultra-thin fluorescent emissive layers and realized the expansion of RZ by adjusting the thickness of MADN and electron transport layer of TPBi, the value of CCT changed from 6932 K to 3072 K, which was not enough to achieve color tunability that simulates sun-light style lighting, and the maximum current efficiency was even less than 10 $cd \cdot A^{-1}$ [20]. Jou *et al.* inserted two hole-modulation-layers (HMLs) between the fluorescence layers, and by changing their thickness, the CCT range of the optimal device was 2400 - 18,000 K, which was enough to cover the CCT span of sunlight on earth, but its maximum power efficiency was still less than 10 $lm \cdot W^{-1}$ [6] [21]. Due to the lack of phosphorescent materials, the efficiency of the above-mentioned CT-WOLEDs was relatively low. Ying et al demonstrated high efficiency and low efficiency roll-off CT-OLED by inserting an ultra-thin red emissive layer in different positions of the blue emissive layer consisting of a phosphorescence-doped exciplex system, the maximum current efficiency reached 34.4 $cd \cdot A^{-1}$, but ΔCCT needed to be further improved [22]. Since the excip-

lex-host system is effective to improve the efficiency of CT-OLED, our experiments also choose this kind of device structure, which contains the exciplex-host material (mCP:PO-T2T) in emitting layer (EML). Different from changing RZ by inserting the spacer layer or changing the position of the red emissive layer, we plan to change RZ by changing the thickness of the red emissive layer and the doping concentration of the material in EML, so as to expand the variation range of CCT.

In this paper, a series of dichromatic color-tunable white phosphorescent OLED devices are fabricated. The device consists of a red emissive layer (R-EML) and two blue emissive layers (B-EML1 and B-EML2). The two blue emissive layers with different phosphorescent doping concentrations in different positions can cover RZ to the maximum extent, and the influence of the change of RZ on the device performance is investigated. mCP:PO-T2T is used as the mixed host material in the emissive layers to achieve maximum RZ expansion, and mCP of different thicknesses are used as spacers between the sub-EMLs to control the energy transfer between them. The change of doping concentration of blue phosphorescent guest material in B-EML1 and doping ratio of PO-T2T in R-EML can adjust the position of RZ and affect the intensity of blue light. In addition, the change of R-EML thickness can also affect the blue luminescence intensity. The change direction and range of CCT of CT-OLED devices are investigated in the above three ways.

2. Sample Preparation and Measurement

All the devices in this experiment are prepared by the thermal evaporation method in a vacuum chamber under a pressure below 5×10^{-4} Pa and based on glass substrates coated with indium tin oxide (ITO) with a surface square resistance of 15 $\Omega \cdot sq^{-1}$. The ITO glass substrates are cleaned by the ultrasonic wave in detergent solution, deionized water, ethanol, and isopropyl alcohol in sequence before use, and cleaned for 10 min in each process, then dried and cooled for 30 min, respectively. In the process of evaporation, all organic materials are deposited on the substrates at a rate of 0.005 - 0.2 $nm \cdot s^{-1}$. The evaporation rate of guest organic materials is adjusted according to the doping ratio of host and guest organic materials, and the evaporation rate of cathode aluminum is 0.3 $nm \cdot s^{-1}$. The evaporation rate and deposition thickness of all materials are measured by four quartz crystal oscillators. The electro-optical properties and electroluminescence (EL) spectra of the devices are obtained by Keithley 2400 Source Meter and PR655 spectroradiometer.

In order to explore the influence of energy distribution in different EMLs and energy transfer on the color-tunable performance of CT-OLED devices, four dichromatic white phosphorescent devices are prepared, whose basic structure is as follows: ITO (100 nm)/HAT-CN (10 nm)/TAPC (30 nm)/mCP (10 nm)/B-EML1 (2 nm)/mCP (3 nm)/B-EML2 (2 nm)/mCP (1 nm)/R-EML (d nm)/PO-T2T (2 nm)/TmPyPB (40 nm)/Liq (2 nm)/Al (100 nm), as shown in **Figure 1**. The doping

concentration (x%) of FIrpic in B-EML1 ($mCP_{1/2}$:PO-$T2T_{1/2}$:x%FIrpic) of device B is 10%, and that of the other three devices is 5%. The thickness (d nm) of R-EML (mCP_{1-y}:PO-$T2T_y$:1%$Ir(piq)_2(acac)$) of device C is 1 nm, and that of the other three devices is 2 nm. The doping ratio (y) of PO-T2T in R-EML of device D is 2/3, and that of the other three devices is 1/2. The B-EML2 ($mCP_{1/2}$:PO-$T2T_{1/2}$:10% FIrpic) is identical for all four devices. The blue and red phosphorescent guest materials in the devices are Bis[2-(4,6-difluorophenyl) pyridinato-C2,N](picolinato)iridium(III) (FIrpic) and Bis(1-phenyl-isoquinoline-C2,N) (Acetylacetonato)iridium(III) ($Ir(piq)_2(acac)$), respectively. 1,3-Di-9-carbazolylbenzene (mCP) and 2,4,6-Tris[3-(diphenylphosphinyl)phenyl]-1,3,5-triazine (PO-T2T) are used as host materials in three sub-EMLs, as spacer layer and carrier transport layer materials at the same time. For hole transport layer (HTL) and electron transport layer (ETL), 4,4'-cyclohexylidenebis[N,N-bis(p-tolyl)aniline] (TAPC) and 1,3,5-tri[(3-pyridyl)-phen-3-yl]benzene (TmPyPB) are selected, respectively. 2,3,6,7,10,11-Hexaaza-triphenylenehexacabonitrile (HAT-CN) and Lithium8-Hydroxyquinolinolate (Liq) are employed as hole injection and electronic injection materials, respectively. The molecular structure of part materials is shown in **Figure 1**.

3. Results and Discussion

Figure 2 and **Table 1** show the electro-optical data of all devices. **Figure 2(a)** shows the current efficiency and power efficiency versus current density curves. **Figure 2(b)** shows the current density and luminance versus voltage curves. As can be seen from **Figure 2** and **Table 1**, although the maximum current efficiency (CE_{max}) and power efficiency (PE_{max}) of device C are the highest among all

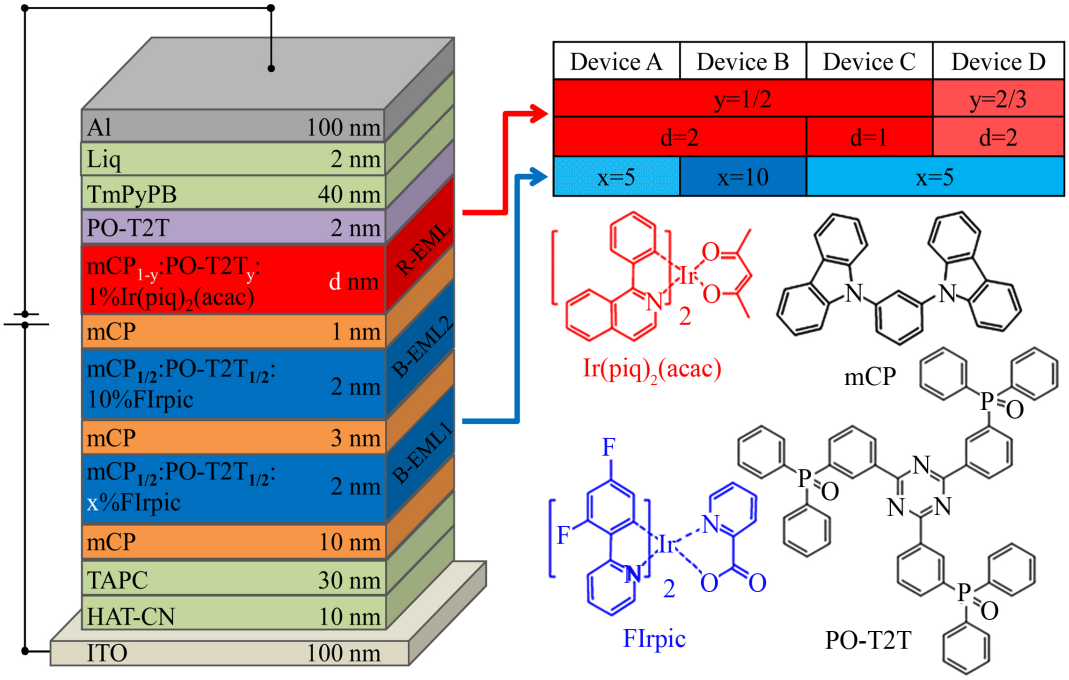

Figure 1. Schematic diagram of the structure of devices A-D and molecular structure of part materials.

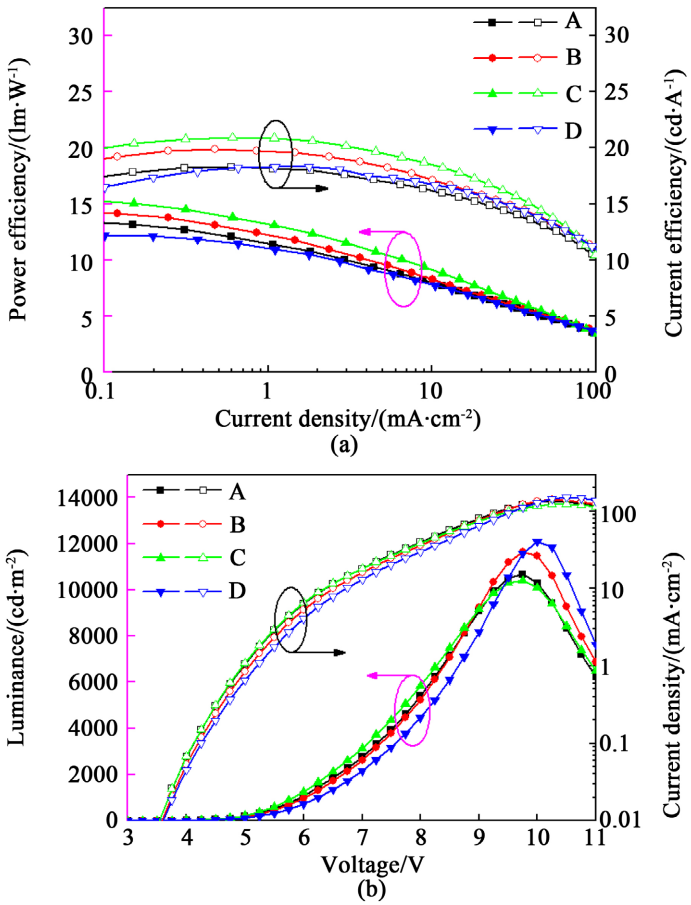

Figure 2. Property curves of devices with different structure. (a) Power efficiency-current density-current efficiency curves; (b) Luminance-voltage-current density curves.

devices, reaching 20.89 cd·A^{-1} and 15.67 lm·W^{-1}, respectively, the maximum current density (CD_{max}) of that is the lowest, only 123.81 mA·cm^{-2}, so the maximum luminance (L_{max}) of device C is only 10,400 cd·m^{-2}. Among the four devices, device D has the largest maximum current density and thus the highest maximum luminance of 152.63 mA·cm^{-2} and 12100 cd·m^{-2}, respectively. This is because PO-T2T is an electron transport material with high electron mobility, its electron mobility (1.7×10^{-3} - 4.4×10^{-3} cm^2/(v·s)) is much higher than electron mobility (3.4×10^{-5} cm^2/(v·s)) and hole mobility (1.2×10^{-4} cm^2/(v. s)) of mCP [23] [24] [25], by increasing the doping ratio of PO-T2T in the R-EML, device D achieves the largest maximum current density and highest maximum luminance.

Figure 3 and Table 1 show the electroluminescence (EL) spectral data for all devices. Figure 3(a) shows normalized curves of the EL spectra of different devices at 9.75 V. Figures 3(b)-(e) are normalized curves of EL spectra of devices A-D at different voltages. Figure 3(f) shows the position of the main maximum luminance (RZ) of different devices in the emitting layer. It can be seen from Figures 3(b)-(e) that the red spectral intensity of all devices is saturated, this is because the red phosphorescent material $Ir(piq)_2(acac)$ has limited doping, thus

Table 1. Electroluminescence characteristics of devices with different structure.

Device	CD_{max}/ (mA·cm^{-2})	L_{max}/ (cd·m^{-2})	CE_{max}/ (cd·A^{-1})	PE_{max}/ (lm·W^{-1})	*CCT*/K		Δ*CCT*/ K	$CIE_{x,y}$	
					3.75 V	9.75 V		3.75 V	9.75 V
A	134.89	10670	18.30	13.58	4106	9036	4930	(0.36, 0.33)	(0.26, 0.34)
B	141.38	11650	19.87	14.54	3728	8816	5088	(0.37, 0.34)	(0.26, 0.35)
C	123.81	10400	20.89	15.67	5765	10725	4960	(0.32, 0.34)	(0.23, 0.35)
D	152.63	12100	18.34	12.30	2661	8407	5746	(0.42, 0.34)	(0.27, 0.35)

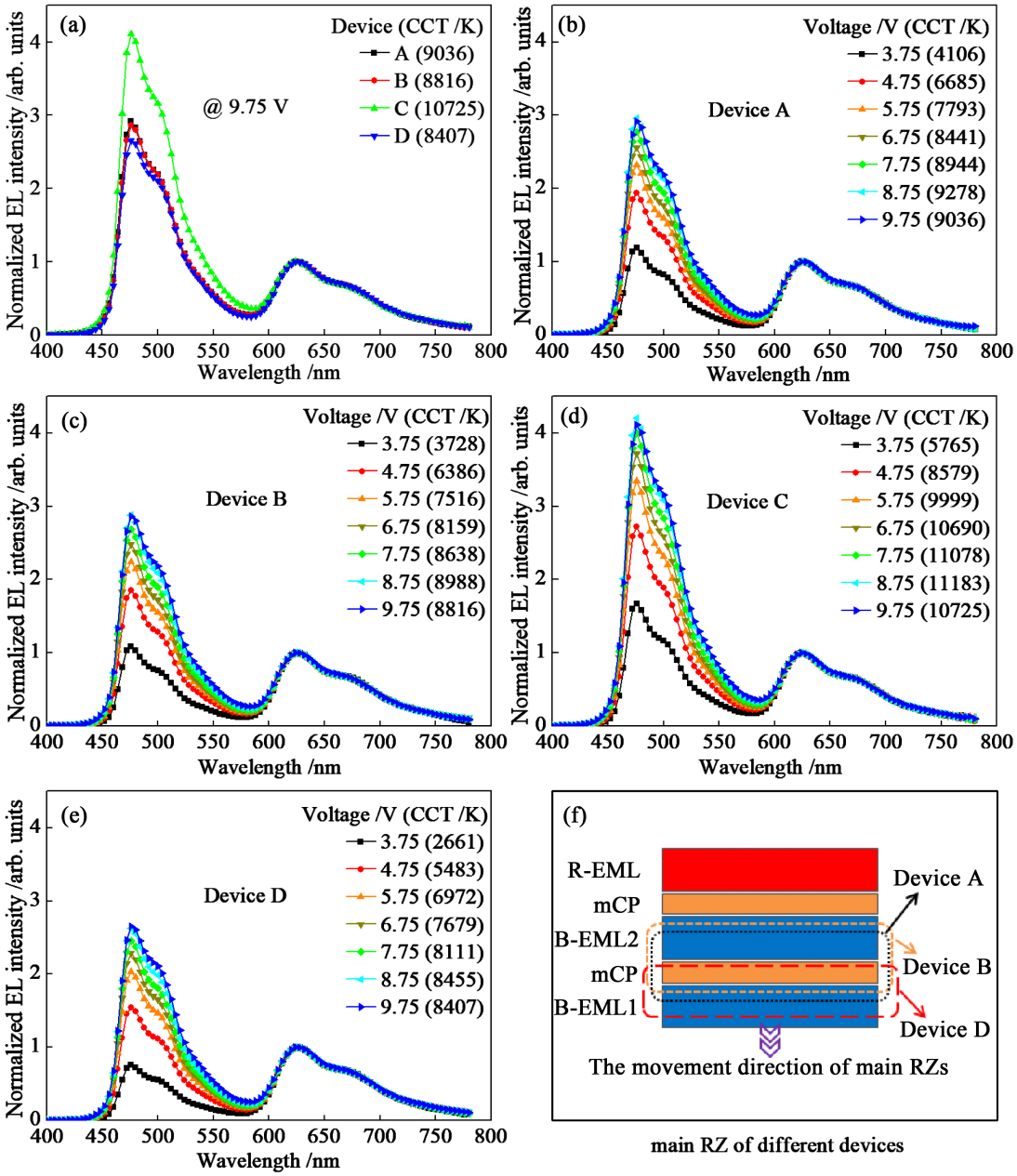

Figure 3. Normalized EL spectra of devices A-D and schematic diagram of the position of the main RZs. (a) Normalized EL spectra of different devices @ 9.75 V; (b) Device A; (c) Device B; (d) Device C; (e) Device D; (f) The position of the main RZ of different devices.

the number of excitons that can be used is small. In addition, PO-T2T is an electron transport material with high electron mobility, thus RZ of all devices move in the HTL direction as the voltage increases, as shown in **Figure 3(f)**. As RZ moves away from the R-EML, the decrease of Dexter energy transfer leads to further saturation of red spectral intensity. As the voltage increases, more excitons are utilized by FIrpic, and the CCT of the devices changes greatly. Increasing the doping concentration of FIrpic in B-EML1 is equivalent to indirectly reducing the doping ratio of PO-T2T, which is opposite to directly increase the doping ratio of PO-T2T in R-EML. Therefore, the main RZ of device B and device D move in the opposite direction compared with device A, the former moves to the side of ETL, and the latter moves to the side of HTL. First, the main RZ of device A and device B always covers B-EML1 and B-EML2. Due to the different doping concentrations of FIrpic in B-EML1 and B-EML2 of device A, which are 5% and 10% respectively, the energy utilization of the B-EML1 of device A is not as high as that of B-EML2. By increasing the doping concentration of FIrpic in the B-EML1 of device B from 5% to 10%, the main RZ can be moved to the side of ETL. And the area covered the B-EML2 is increased, which can improve the utilization of FIrpic, and thus enhance the intensity of blue light. However, because RZ is closer to R-EML, the Dexter energy transfer from B-EML2 to R-EML is increased, resulting in the blue spectral intensity actually decreasing compared with the red light. Therefore, the CCT of device B is lower than that of device A at both low and high voltages, which are (3728K @ 3.75V) and (8816k @ 9.75V), respectively. Secondly, the increase of PO-T2T doping ratio in the R-EML pushes the main RZ towards the side of HTL, which of device D only covers the B-EML1. Compared with device A, although the mCP spacer of 3 nm can effectively block the energy transfer from B-EML1 to R-EML, the doping concentration of FIrpic in B-EML1 (5%) is only half of that in B-EML2, so the blue spectral intensity of device D decreases significantly, and the CCT of which at low and high voltages is not only lower than that of device A, but even lower than that of device B, are (2661 K @ 3.75V) and (8407 K @ 9.75V), respectively, corresponding to the Commission Internationale de L'Eclairage ($CIE_{x,y}$) coordinates (0.42, 0.34) and (0.27, 0.35), respectively. The maximum power efficiency (PE_{max}) of device D is the lowest among the four devices, only 12.30 $lm \cdot W^{-1}$, which also indicates that the energy utilization of device D is not high. However, as the voltage varies from 3.75 V to 9.75 V, the ΔCCT of device D is the widest, reaching 5746 K (2661 - 8407 K). Finally, due to the reduction of the R-EML thickness to 1 nm, the red phosphorescent material $Ir(piq)_2(acac)$ is also reduced by half, so it's easier to saturate, resulting in a significant increase in the CCT of the device at low and high voltages, reaching 5765 K @ 3.75 V and 10,725 K @ 9.75 V, respectively, the ΔCCT (4960 K) is narrower than that of device D.

4. Conclusion

ΔCCT is an important parameter to measure the performance of CT-OLED. In

this paper, a series of dichromatic white phosphorescent CT-OLED devices are prepared, and the effect of the number of phosphorescent materials and the position of RZ on the change direction and range of CCT is investigated by changing the doping concentration and the thickness of the EML. Increasing the amount of blue phosphorescent material FIrpic (e.g. device B) or decreasing the amount of red phosphorescent material $Ir(piq)_2(acac)$ (e.g. device C) will only affect the change direction of CCT, but not enough to expand the range of CCT. In order to achieve a wider range of color adjustment, the position change of the main RZ and the energy transfer effect between different color EMLs should be considered comprehensively. The device D achieves the best electro-optical and spectral characteristics, with the widest ΔCCT of 5746 K (@ 3.75 V~9.75 V), maximum current efficiency, and luminance of 18.34 $cd \cdot A^{-1}$ and 12,100 $cd \cdot m^{-2}$, respectively. The change of doping concentration and thickness of EML can affect the position of RZ, and then affect the direction and change range of CCT. In addition, expanding the range of RZ in EML and controlling the energy transfer process between different sub-EMLs should help to further improve ΔCCT, which needs to be further studied.

Conflicts of Interest

The authors declare no conflicts of interest regarding the publication of this paper.

References

[1] Jeong, C., Park, Y.B. and Guo, L.J. (2021) Tackling Light Trapping in Organic Light-Emitting Diodes by Complete Elimination of Waveguide Modes. *Science Advances*, **7**, eabg0355. https://doi.org/10.1126/sciadv.abg0355

[2] Wang, Q., Bai, J.W., Zhao, C.B., *et al*. (2021) Simplified Dopant-Free Color-Tunable Organic Light-Emitting Diodes. *Applied Physics Letters*, **118**, Article ID: 253301. https://doi.org/10.1063/5.0042087

[3] Solanki, A., Awasthi, A., Unni, K.N.N., *et al*. (2021) An Efficient and Facile Method to Develop Defect-Free OLED Displays. *Semiconductor Science and Technology*, **36**, Article ID: 065005. https://doi.org/10.1088/1361-6641/abf3a8

[4] Wang, D.X., Hauptmann, J., May, C., *et al*. (2021) Roll-to-Roll Fabrication of Highly Transparent Ca:Ag Top-Electrode towards Flexible Large-Area OLED Lighting Application. *Flexible and Printed Electronics*, **6**, Article ID: 035001. https://doi.org/10.1088/2058-8585/abf159

[5] Jung, S.W., Kim, K.S., Park, H.U., *et al*. (2021) Patternable Semi-Transparent Cathode Using Thermal Evaporation for OLED Display Applications. *Advanced Electronic Materials*, **7**, Article ID: 2001101. https://doi.org/10.1002/aelm.202001101

[6] Jou, J.H., Shen, S.M., Wu, M.H., *et al*. (2011) Sunlight-Style Organic Light-Emitting Diodes. *Journal of Photonics for Energy*, **1**, Article ID: 011021. https://doi.org/10.1117/1.3583640

[7] Mao, M., Lam, T.L., To, W.P., *et al*. (2021) Stable, High-Efficiency Voltage-Dependent Color-Tunable Organic Light-Emitting Diodes with a Single Tetradentate Platinum(II) Emitter Having Long Operational Lifetime. *Advanced Materials*, **33**, Article ID: 2004873. https://doi.org/10.1002/adma.202004873

[8] Brainard, G.C., Hanifin, J.P., Warfield, B., *et al*. (2015) Short-Wavelength Enrichment of Polychromatic Light Enhances Human Melatonin Suppression Potency. *Journal of Pineal Research*, **58**, 352-361. https://doi.org/10.1111/jpi.12221

[9] Arthur, J.N., Forrestal, D.P., Woodruff, M.A., *et al*. (2018) Facile and Dynamic Color-Tuning Approach for Organic Light-Emitting Diodes Using Anisotropic Filters. *ACS Photonics*, **5**, 2760-2766. https://doi.org/10.1021/acsphotonics.8b00527

[10] Yu, J.S. and Zhong, J. (2018) Introduction to OLED Display Technology. Science Press, Beijing, 181-185.

[11] Burrows, P.E., Forrest, S.R., Sibley, S.P., *et al*. (1996) Color-Tunable Organic Light-Emitting Devices. *Applied Physics Letters*, **69**, 2959-2961. https://doi.org/10.1063/1.117743

[12] Lee, J., Koh, T.W., Cho, H., *et al*. (2015) Color Temperature Tuning of White Organic Light-Emitting Diodes via Spatial Control of Micro-Cavity Effects Based on Thin Metal Strips. *Organic Electronics*, **26**, 334-339. https://doi.org/10.1016/j.orgel.2015.08.002

[13] Zhang, J.H., Song, J.T., Zhang, H., *et al*. (2016) Sunlight-Like White Organic Light-Emitting Diodes with Inorganic/Organic Nanolaminate Distributed Bragg Reflector (DBR) Anode Microcavity by Using Atomic Layer Deposition. *Organic Electronics*, **33**, 88-94. https://doi.org/10.1016/j.orgel.2016.03.010

[14] Jiang, J.X., Zheng, W.Y., Chen, J.F., *et al*. (2020) Color-Tunable Organic Light Emitting Diodes for Deep Blue Emission by Regulating the Optical Micro-Cavity. *Molecules*, **25**, Article 2867. https://doi.org/10.3390/molecules25122867

[15] Frobel, M., Schwab, T., Kliem, M., *et al*. (2015) Get It White: Color-Tunable AC/DC OLEDs. *Light-Science & Applications*, **4**, e247. https://doi.org/10.1038/lsa.2015.20

[16] Joo, C.W., Moon, J., Han, J.H., *et al*. (2014) Color Temperature Tunable White Organic Light-Emitting Diodes. *Organic Electronics*, **15**, 189-195. https://doi.org/10.1016/j.orgel.2013.10.005

[17] Lee, H., Cho, H., Byun, C.W., *et al*. (2018) Color-Tunable Organic Light-Emitting Diodes with Vertically Stacked Blue, Green, and Red Colors for Lighting and Display Applications. *Optics Express*, **26**, 18351-18361. https://doi.org/10.1364/OE.26.018351

[18] Jeon, Y., Noh, I., Seo, Y.C., *et al*. (2020) Parallel-Stacked Flexible Organic Light-Emitting Diodes for Wearable Photodynamic Therapeutics and Color-Tunable Optoelectronics. *ACS Nano*, **14**, 15688-15699. https://doi.org/10.1021/acsnano.0c06649

[19] Choi, S., Kang, C.M., Byun, C.W., *et al*. (2020) Thin-Film Transistor-Driven Vertically Stacked Full-Color Organic Light-Emitting Diodes for High-Resolution Active-Matrix Displays. *Nature Communications*, **11**, Article No. 2732. https://doi.org/10.1038/s41467-020-16551-8

[20] Xu, T., Yang, M.J., Liu, J., *et al*. (2016) Wide Color-Range Tunable and Low Roll-Off Fluorescent Organic Light Emitting Devices Based on Double Undoped Ultrathin Emitters. *Organic Electronics*, **37**, 93-99. https://doi.org/10.1016/j.orgel.2016.06.014

[21] Jou, J.H., Wu, M.H., Shen, S.M., *et al*. (2009) Sunlight-Style Color-Temperature Tunable Organic Light-Emitting Diode. *Applied Physics Letters*, **95**, Article ID: 013307. https://doi.org/10.1063/1.3176217

[22] Ying, S., Wu, Y.B., Sun, Q., *et al*. (2019) High Efficiency Color-Tunable Organic Light-Emitting Diodes with Ultra-Thin Emissive Layers in Blue Phosphor Doped Exciplex. *Applied Physics Letters*, **114**, Article ID: 033501. https://doi.org/10.1063/1.5082011

[23] Hung, W.Y., Fang, G.C., Lin, S.W., *et al*. (2014) The First Tandem, All-Exciplex-Based WOLED. *Scientific Reports*, **4**, Article No. 5161. https://doi.org/10.1038/srep05161

[24] Lee, J.H., Cheng, S.H., Yoo, S.J., *et al*. (2015) An Exciplex Forming Host for Highly Efficient Blue Organic Light Emitting Diodes with Low Driving Voltage. *Advanced Functional Materials*, **25**, 361-366. https://doi.org/10.1002/adfm.201402707

[25] Tsuboi, T., Liu, S.W., Wu, M.F., *et al*. (2009) Spectroscopic and Electrical Characteristics of Highly Efficient Tetraphenylsilane-Carbazole Organic Compound as Host Material for Blue Organic Light Emitting Diodes. *Organic Electronics*, **10**, 1372-1377. https://doi.org/10.1016/j.orgel.2009.07.020